

4 Cold Dark Matter Search with XENON and DARWIN

Laura Baudis, Peter Barrow, Sandro D’Amato, Domenico Franco, Michelle Galloway, Andrea Gmuer, Gaudenz Kessler, Alexander Kish, Andreas James, Daniel Mayani, Francesco Piastra, Julien Wulf and Yuehuan Wei

in collaboration with: Albert Einstein Center for Fundamental Physics Bern, Columbia University, UCLA, INFN, University of Münster, Coimbra University, Subatech, The Weizmann Institute of Science, University of Mainz, SJTU, MPIK Heidelberg, Stockholm University, Rice University, University of Chicago, University of Bologna, Nikhef, Purdue University, NYU of Abu Dhabi

(XENON Collaboration)

After decades of increasingly precise astronomical observations, we have unequivocal evidence that the matter forming galaxies, clusters of galaxies and the largest observed structures in the universe is mostly non-luminous, or dark. These observations include galactic rotation curves, orbital velocities of individual galaxies, cluster masses from gravitational lensing, cosmic microwave background acoustic fluctuations, the abundance of light elements, and the mapping of large scale structures. Cosmological simulations based on the Λ CDM model do predict the observed large-scale structures in the universe. In this model, which so far provides the only paradigm that can explain all observations, our universe is spatially flat and composed of $\sim 5\%$ atoms, $\sim 27\%$ dark matter and $\sim 68\%$ dark energy [1].

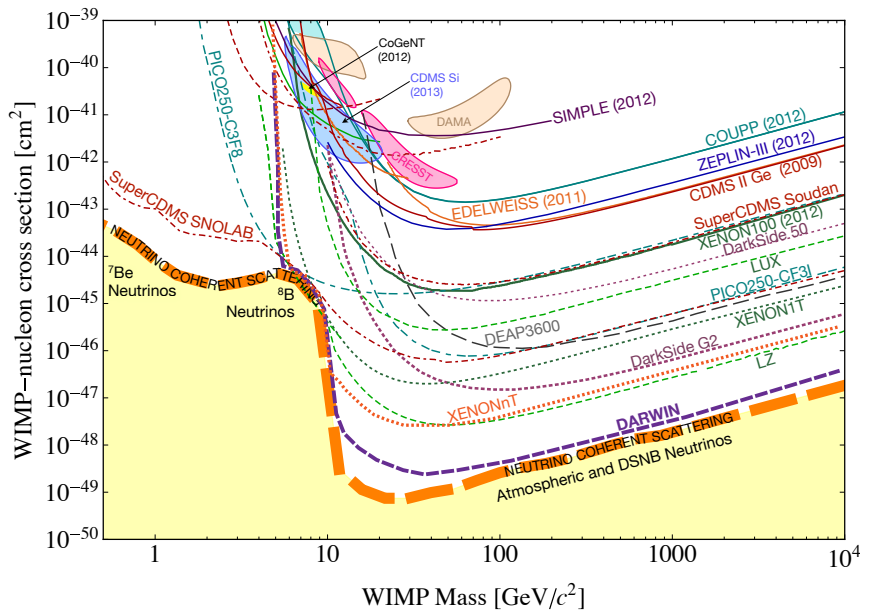
Understanding the nature of dark matter poses a significant challenge to astroparticle physics. Its solution may involve new particles with masses and cross sections characteristic of the electroweak scale, so-called Weakly Interacting Massive Particles (WIMPs). WIMPs may be directly detected by scattering off nuclei in ultra-sensitive

laboratory detectors [2]. Since the predicted cross sections and hence expected signal rates are very low, large detector masses and extremely low backgrounds are necessary ingredients of any experiment aiming to discover WIMPs [3]. Existing upper limits and projected sensitivities for the spin-independent WIMP-nucleon interaction cross section as a function of the WIMP mass are summarized in Fig. 4.1.

Liquid xenon offers an excellent medium for building non-segmented, homogeneous, compact and self-shielding dark matter detectors: it is a good scintillator and ionizer in response to the passage of radiation, and the simultaneous detection of ionization and scintillation signals allows to identify the primary particle interacting in the liquid. In addition, the 3D position of an interaction can be determined with sub-mm (in the z-coordinate) to mm (in the x-y-coordinate) precisions in a time projection chamber (TPC), where the prompt light (S1) and charge (S2, in general via proportional scintillation) signals are detected. These features, together with the relative ease of scale-up to large masses, have contributed

FIG. 4.1 –

Spin-independent WIMP-nucleon scattering results: Existing limits from the ZEPLIN-III [4], XENON10 [5], XENON100 [6], and LUX [7] experiments, along with projections for DarkSide-50 [8], LUX [7], DEAP3600 [9], XENON1T, DarkSide G2, XENONnT, LZ [10], and DARWIN [11]. DARWIN is designed to probe the entire parameter region for WIMP masses above $\sim 6 \text{ GeV}/c^2$, until the neutrino background (yellow region) will start to dominate the recoil spectrum. Experiments based on the mK cryogenic technique such as SuperCDMS [12] and EURECA [13] have access to lower WIMP masses. Adapted from [14].



to make LXe a powerful target for WIMP searches [15]. The dual-phase LXe TPCs ZEPLIN-III [4, 16], XENON10 [5], XENON100 [6, 17] and LUX [7] are successful implementations of the technique. XENON1T, the next step of the XENON program, is in construction at LNGS. The next phase in the LUX program, LUX-ZEPLIN (LZ), foresees a 7 t LXe detector at SURF, with the goal of reaching a sensitivity of $2 \times 10^{-48} \text{ cm}^2$ after three years of data taking [10]. The upgrade of XENON1T, XENONnT, is to reach a similar sensitivity, with planned operation between 2018-2021. DARK matter Wimp search with Noble liquids (DARWIN) is an initiative to build an ultimate, multi-ton dark matter detector at LNGS [11, 18], to probe the spin-independent WIMP-nucleon cross section down to the 10^{-49} cm^2 region. It would thus explore the experimentally accessible parameter space, which eventually be limited by irreducible neutrino backgrounds.

4.1 The XENON dark matter program

The primary goal of the XENON program is to directly detect WIMP dark matter in ultra-sensitive low-background detectors. XENON100 is a 161 kg double-

phase Xe TPC, still in operation at the Gran Sasso Laboratory (LNGS), for calibration measurements and R&D for the next phase of the project. XENON1T is in an advanced construction stage in hall B of LNGS. All its major components have been designed such that an upgrade to a detector which is at least twice more massive is rather straight-forward. For this stage of the program, called XENONnT, the main challenges will be to develop a new, larger TPC and to lower the backgrounds further. With a planned exposure of $\sim 20 \text{ t} \times \text{y}$ the expected sensitivity is roughly one order of magnitude below the one of XENON1T, shown schematically in Fig.4.2.

XENON1T houses a $\sim 3.3 \text{ t}$ LXe, of which 2.0 t constitute the active mass of the dual-phase TPC. The background goal is less than one event in $2 \text{ t} \times \text{y}$ in the central fiducial region of $\sim 1.0 \text{ t}$ which leads to a sensitivity to spin-independent WIMP-nucleon cross sections of $2 \times 10^{-47} \text{ cm}^2$ for $50 \text{ GeV}/c^2$ WIMPs.

The underground building, the Cherenkov muon veto, the cryostat support, the outer and inner cryostats, as well as the xenon storage, purification and recovery systems are in place, see Fig. 4.3. The TPC is under construction, first cryogenic tests will be performed at UZH; its assembly at LNGS is planned for summer 2015. After the detector commissioning first data is to be acquired within that same year.

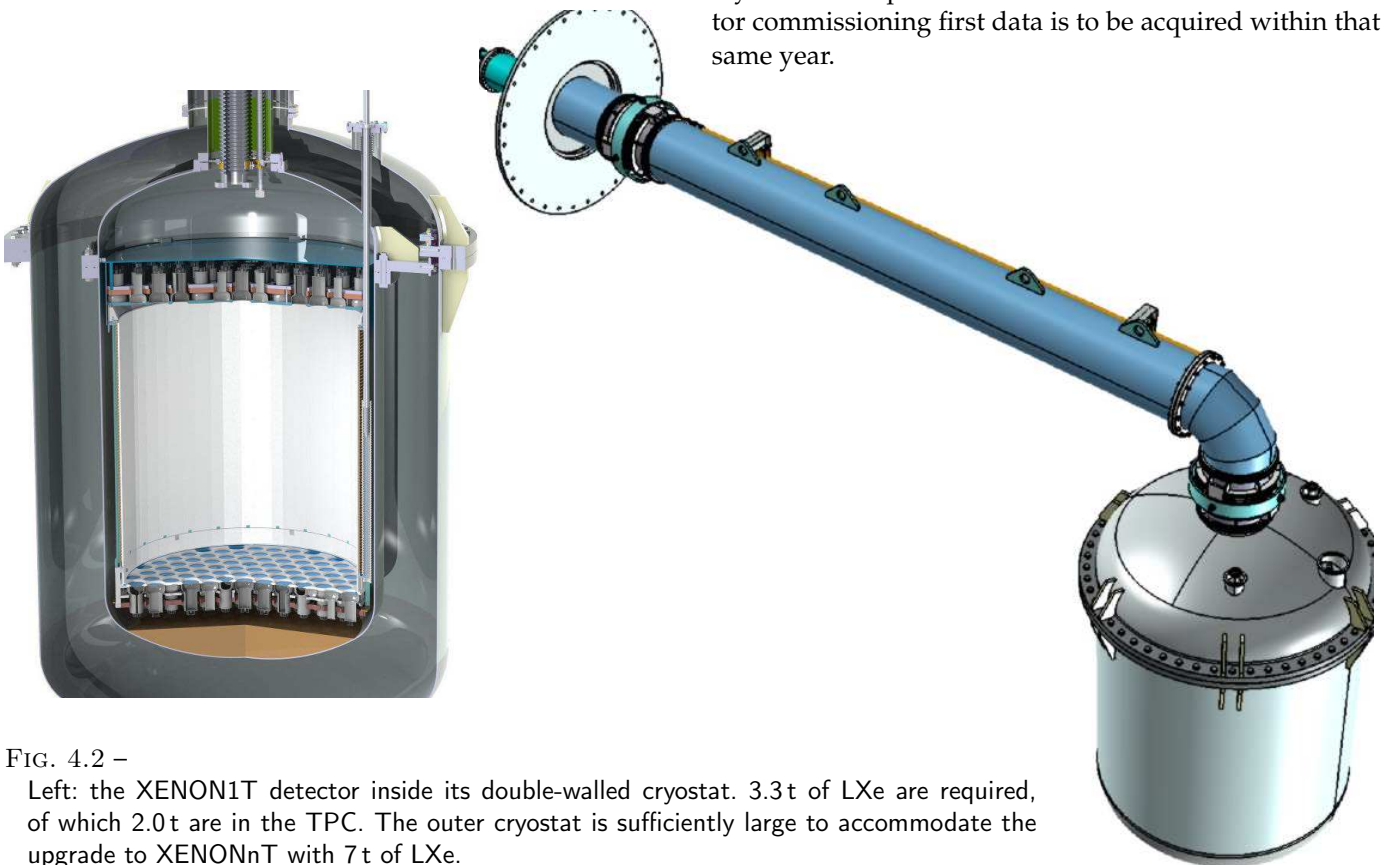


FIG. 4.2 –

Left: the XENON1T detector inside its double-walled cryostat. 3.3 t of LXe are required, of which 2.0 t are in the TPC. The outer cryostat is sufficiently large to accommodate the upgrade to XENONnT with 7 t of LXe.

Right: the detector with its single connecting pipe, containing both the transmission lines for gaseous and liquid xenon and all electronic cables.

FIG. 4.3 –

Left: the XENON1T inner and outer cryostats are installed underground at LNGS, inside a 9.6 m diameter water Cherenkov muon veto.

Right: The main underground infrastructures, as well as the building with DAQ, xenon storage, purification and cryogenic systems are in place.



4.2 Analysis of XENON100 science data

We participate in various aspects of the analysis of the XENON100 data, from the development of data quality and physics cuts, to the final physics analysis. Our current focus is on inelastic WIMP-nucleus scatters, on the search for bosonic SuperWIMPs, on background studies of the latest, still blinded, dark matter run, and on the YBe and $^{83\text{m}}\text{Kr}$ calibrations.

4.2.1 Inelastic analysis

In collaboration with theorists from Darmstadt, we worked out the signature of dark matter scattering inelastically off xenon nuclei, where the nucleus is excited to a low-lying state with subsequent fast de-excitation $\text{Xe}^* \rightarrow \text{Xe} + \gamma$ (39.6 keV). The observation of both elastic and inelastic channels in a xenon detector could provide information on the nature of the interaction, on the mass of the dark matter particle and eventually on the dark matter halo, as the two channels probe different regions of the dark matter velocity distribution [19].

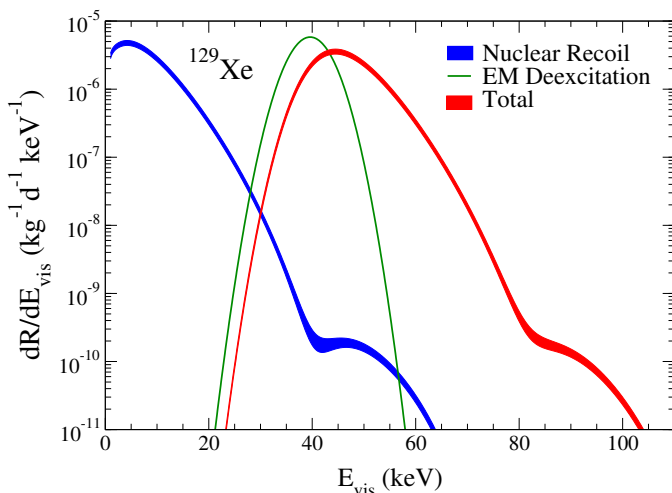


FIG. 4.4 – Decomposition of the energy spectrum for inelastic scattering off ^{129}Xe (see text) assuming a 100 GeV WIMP with $\sigma_{\text{nucleon}} = 10^{-40} \text{ cm}^2$, see [19].

In Fig.4.4, we show the expected components of the energy spectrum for inelastic scattering off ^{129}Xe . We are working on the analysis of the latest XENON100 physics data, where we study the total deposited energies in the S2 and S1 planes. The signal region is determined with AmBe neutron calibration data, see Fig.4.5. Since the search window differs from our standard WIMP analysis, we developed new cuts and studied their efficiency. We are performing a maximum likelihood analysis to determine the sensitivity of XENON100, which reaches down to $4.8 \times 10^{-38} \text{ cm}^2$ for 100 GeV WIMPs, improving upon earlier results by XMASS [20].

4.2.2 Bosonic SuperWIMPs

Bosonic SuperWIMPs are light (10-100 keV), superweakly interacting dark matter candidates [21]. In the XENON100 detector, these could be observed via the axio-electric effect, where a SuperWIMP would be completely absorbed by a xenon atom, depositing an energy in the detector approximately equal to its rest mass. Such a signal would thus be found within the electronic re-

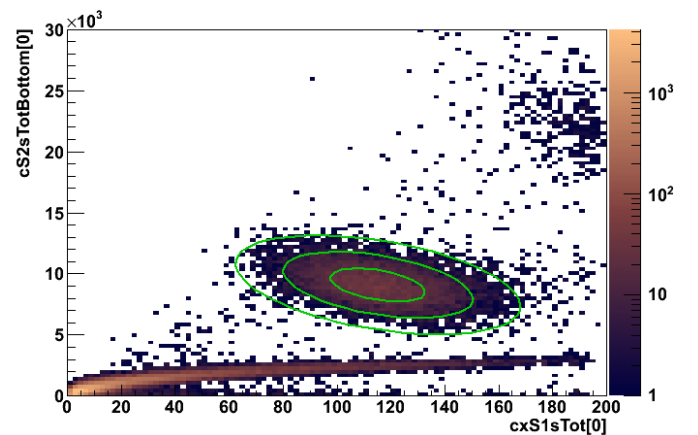


FIG. 4.5 – The signal region in S2 versus S1, determined with AmBe neutron calibration data with a two-dimensional Gaussian fit. The green ellipses indicate the 1-, 2- and 3- σ contours (for 39.6 keV γ + NR).

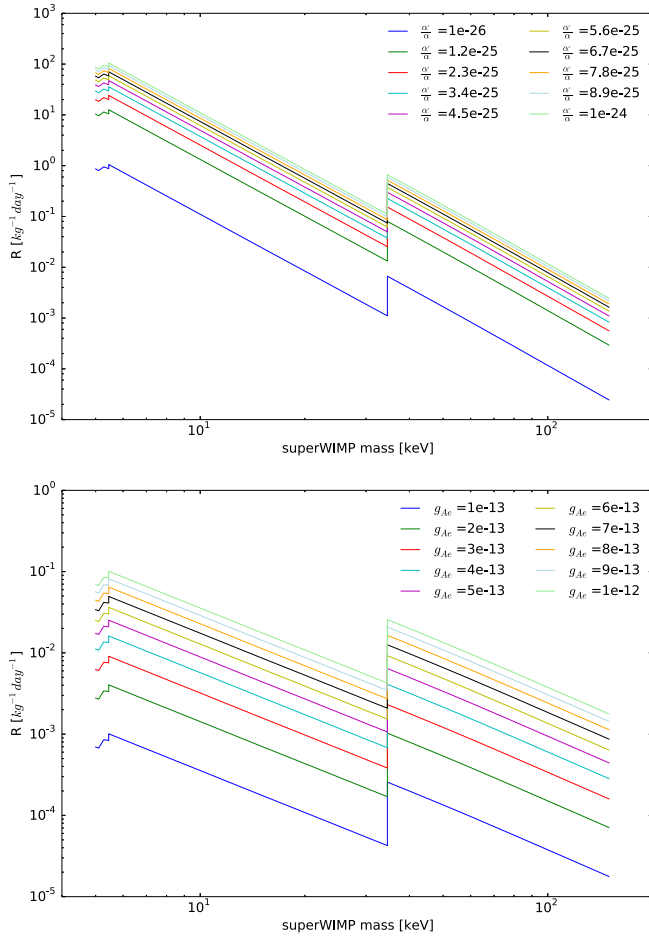


FIG. 4.6 – Predicted integral rates to be observed in the XENON100 detector for vector (top) and pseudo-scalar (bottom) bosonic SuperWIMPs for a range of couplings to electrons which are not (yet) excluded.

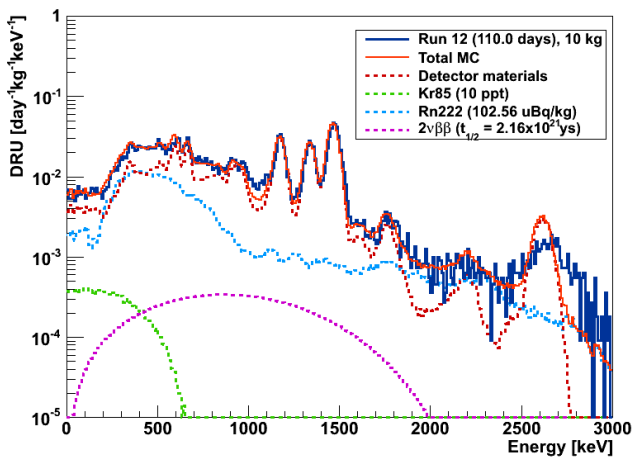


FIG. 4.7 – Measured and simulated energy distributions for a 10 kg LXe fiducial mass in XENON100. The simulation is based on material screening results. The main contributions are from detector materials and internal radon. The contributions from ^{85}Kr and ^{136}Xe decays are also shown.

coil band of events. The rate at which SuperWIMPs interact inside the detector depends on their type (pseudoscalar or vector), their coupling to electrons and their mass [21]. In Fig.4.6 we show the predicted integral rates in XENON100, for an assumed exposure of $225 \text{ d} \times 34 \text{ kg}$. We are analyzing the electronic recoil band of XENON100 for these type of signatures, with the goal of improving upon the sensitivity of XMASS [22] due to a larger exposure, a lower background and an extended energy region for the search. We have defined the physics cuts for the analysis, and are now developing a profile likelihood approach to calculate our sensitivity.

4.2.3 Background analysis

The main sources for the electronic recoil background in the XENON100 detector are radioactive contaminations in the detector materials, the intrinsic ^{222}Rn and ^{85}Kr radioactivity in LXe, and the decays of ^{222}Rn daughters inside the shield cavity. Extensive Monte Carlo simulations of the XENON100 detector were performed by our group with the GEANT4 software, using a detailed geometry and the measured radioactivity of all components [23]. Using this simulation, we are now comparing the predictions with the dark matter data taken during the latest science run, that lasted 153.8 live days. Figure 4.7 shows a preliminary comparison between the data acquired in this run and the MC predictions. To further improve the matching between data and MC, in particular at high energies, the position reconstruction of events in the various selected fiducial volumes is being investigated. Because the PMTs saturate for large S2 signals, this effect can lead to a misplacement of the interaction vertex at high energies, and thus affects the measured rate for a given fiducial volume.

4.3 The XENON1T time projection chamber

We participate in the design, production, assembly, and testing of the XENON1T TPC. The field cage, to be assembled at our institute, is made of high purity copper as the conductor and PTFE as insulator which also acts as an efficient reflector for LXe scintillation light. The TPC is designed with interlocking PTFE panels to account for the contraction when cooled down to -95°C . The cage has a height of 970 mm and a diameter of 960 mm, and may contain an active LXe mass of $\sim 2 \text{ t}$. To achieve a TPC drift field of $0.5 - 1 \text{ kV/cm}$, the cathode at the bottom, made from $200 \mu\text{m}$ wires, will be biased with -50 to -100 kV . The required field homogeneity is obtained with the help of 74 massive field shaping rings made from oxygen-free high conductivity (OFHC) copper. The geometry was optimized by simulation.

The field cage will be subjected to cryogenic and struc-

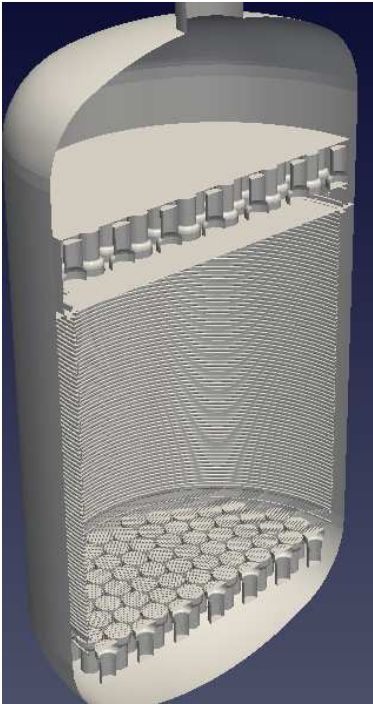


FIG. 4.8 – The implementation of the XENON1T geometry inside the newly developed field simulation software.

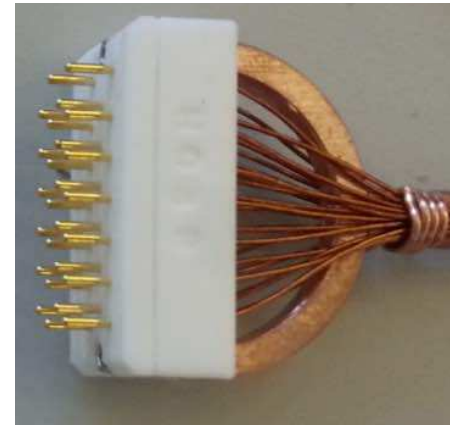
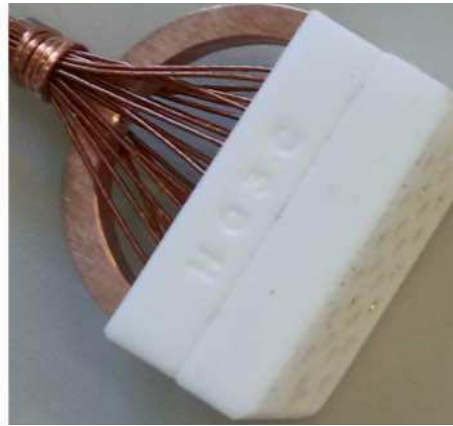


FIG. 4.9 – Custom-made connectors for XENON1T. Above: High voltage connector with Kapton cables and strain relief. Right: Signal coaxial cables with MMCX connectors in a PTFE holder structure.



tural integrity tests in a large dewar that can be cooled down to -95°C . Upon the successful completion of these tests, the cage will be disassembled and shipped to LNGS.

As indicated above, the design of the TPC was based on accurate electric field simulations. We had used the commercial simulation software *COMSOL Multiphysics* to simulate a first, axial symmetrical geometry of the detector. Because more detailed simulations were needed, a new software has been developed by our group. It uses the boundary element method, a numerical solution technique to solve Maxwell's equation and it is mainly based on the Kasper simulation package developed by the KATRIN [24] experiment. We are now able to calculate very large and complex geometries on fast parallelized computing platforms using GPUs. With the iterative Robin Hood [25] methods as charge density solver, the memory consumption has been greatly reduced. With this software, non axial symmetrical geometries of the detector were simulated, leading to the identification of the optimal electrode structures in the TPC. Fig.4.8 shows the implementation of the XENON1T geometry into our simulation software. We will extend it to include particle tracking, with the goal of increasing the reconstruction precisions of an interaction vertex inside the TPC. We will also provide the field corrections maps, needed after the commissioning of the TPC, once data taking starts.

We are responsible for the cables and connectors (signal and HV) on the xenon side, to power the PMTs and

extract the signal from the TPC. Due to strict background requirements of the experiment, and since the cabling will be located near the active volume of the TPC, ultra-low radioactivity cables and connectors are used. For the high voltage, we employ Kapton insulated copper wires connected with custom-made connectors (see Fig.4.9) made of PTFE and copper. The connector was tested to withstand up to 2.0 kV under realistic operating conditions. For the signal cable, a full coaxial connection is provided using PTFE insulated coax cables and MMCX connectors. The bunches of 24 signal cables each are held together by a PTFE structure, as shown in Fig.4.9.

The vacuum feed-throughs, shown in Fig.4.10, are made of epoxy with high thermal conductivity and low out-gassing. These are mounted on the so-called *porcupine*, Fig.4.11, a stainless steel vessel with several CF flanges. This vessel is directly connected to the large cable pipe through a CF100 elbow at the level of the cryogenic room.

In mid 2014, we have installed 900 cables into the pipe that guides them from the top of the TPC through the water tank, to the underground building. Because later access is complicated, we have already installed the required number of cables for XENONnT, including some contingency, as well. At the beginning of 2015, the cables with the feed-throughs were mounted on the porcupine and connected to the cables in the pipe. The porcupine was installed onto the pipe, and all the connections



FIG. 4.10 – Example vacuum feed-throughs for 10 high voltage and 10 signal cables.

were successfully tested. In mid 2015 the last sections of the cables will be connected to the PMT voltage dividers (bases) at UZH, then installed inside the TPC, connected and tested once more.

4.4 The XENON1T PMTs

The final version of the photomultiplier tube selected for XENON1T is the Hamamatsu R11410-21. It has been developed by Hamamatsu with extensive feedback from us regarding the requirements for dark matter searches, based on radioactivity measurements of all production components, and of the final product [26], and extensive tests performed in LXe. It is a 3-inch diameter tube and operates stably at -100°C and 2 atm [27]. Apart from a greatly reduced intrinsic radioactivity level, a major ad-

vantage is its high quantum efficiency (QE) at the xenon scintillation wavelength of 175 nm. With our HPGe facility at LNGS, we have screened 240 out of 283 PMTs. The results are satisfactory for XENON1T [26]. A mean value of $\text{QE} = 35\%$ has been observed with a few tubes reaching 40%. All tubes to be installed in XENON1T are tested at room temperature and at -100°C . Around 10% of them are tested at UZH in LXe to measure their performance in the conditions of a dark matter experiment. The main features that we monitor are the dark count rate, the gain evolution and the afterpulse rate before, during and after each cool down in LXe, which have a typical duration of a few weeks. In XENON1T all PMTs will be equalized in gain with the aim of achieving a peak-to-valley ratio in the SPE spectrum of around 4. This ensures a good separation of the single photoelectron signal from the noise component of the spectrum. As we show in Fig.4.12, this is achieved at gains above 2×10^6 .

After completing the cryogenic tests for the remaining tubes for XENON1T, all PMTs will be mounted on their support structures of the top and bottom arrays, tested once again and then brought to LNGS for integration into the TPC.

18

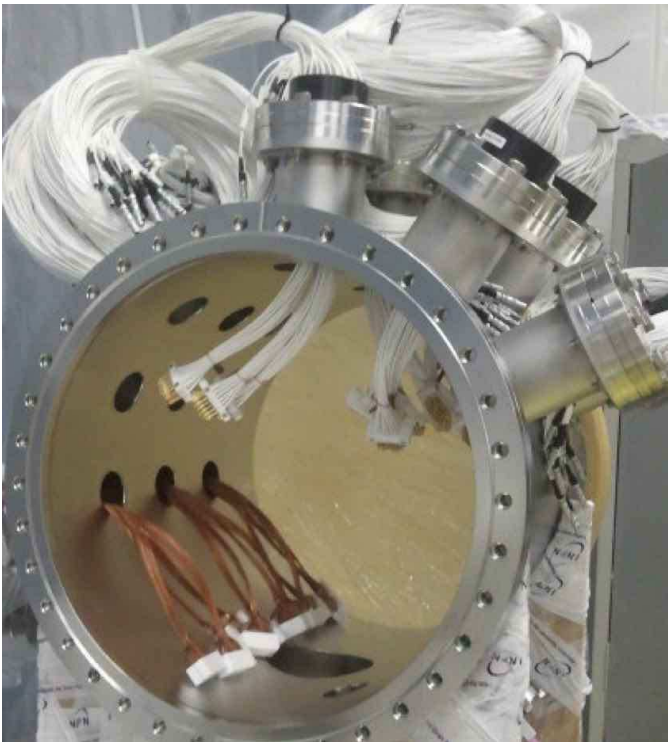


FIG. 4.11 – Porcupine with mounted signal and high voltage feed-throughs (nipples on the side open).

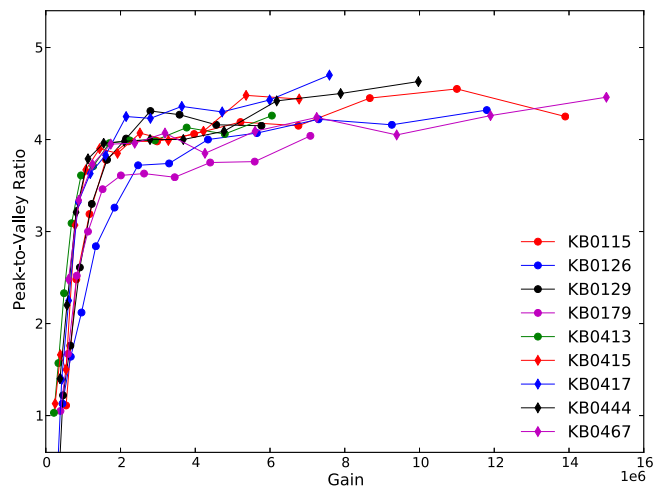


FIG. 4.12 – Peak-to-valley ratio as a function of gain. At a gain of about 2×10^6 the PMTs reach a sufficiently high peak-to-valley ratio.

Several voltage-divider layouts have been tested resulting in a design with a power dissipation of $<0.025\text{ W/PMT}$ showing good linearity over the full DAQ range at low rate. Currently, the printed circuits are being produced. Once these arrive at UZH, we will produce all bases for XENON1T, test them and mount them onto the PMTs. We will also perform final linearity tests.

In the next two years, we will develop the bases for XENONnT, which have even stricter requirements on the radioactivity levels of the components.

4.5 The XENONnT and DARWIN projects

Most major XENON1T components are designed such that a doubling of the detector mass will be feasible once the science goals of XENON1T have been achieved. The underground infrastructure, in particular the water shield, the xenon storage vessel, the cryogenic system, the cryostat support, the outer cryostat vessel and the connection pipe to the building can be reused for XENONnT. The DAQ system for XENON1T is designed such that it can be upgraded for the ~ 200 extra channels of XENONnT without new developments. The main remaining work will be to design and build a new TPC capable of being biased with higher cathode voltages, and to lower the intrinsic backgrounds from radon and krypton further. XENONnT will be developed and various parts will be constructed while XENON1T is taking science data, utilizing the experience gained from the new experiment, and is expected to take science data by 2018.

DARWIN is an ultimate WIMP detector with a sensitivity down to 10^{-49} cm^2 . At these cross-sections, neutrino interactions, which cannot be reduced by target fiducialization, will limit the sensitivity to WIMP interactions [11]. With a target mass of about 20 tons, this project would be the successor of XENONnT, possibly installed inside the XENON1T water tank. Currently our R&D is focused on topics where we have experience from XENON: design and prototyping of the time projection chamber, Monte Carlo simulations of the radioactive background, new light read-out schemes and tests of light sensors in noble liquids, material screening with high-purity germanium spectroscopy, as well as the science impact of the facility. We additionally perform charge and light yield measurements of nuclear and electronic recoils in LXe at low energies, which are necessary to define accurate energy scales in noble liquid dark matter detectors. The R&D and design phase will end by 2019, after which the construction phase of the various sub-systems is to start. The detector would be installed and commissioned underground starting in 2021, with a first science run to start by 2023. The facility would be operated for at least 5 years, thus until 2027, possibly longer.

- [1] Planck Collaboration, *Planck 2015 results. XIII. Cosmological parameters*, (2015) arXiv:1502.01589.
- [2] M.W. Goodman and E. Witten, *Phys. Rev. D* 31 (1985) 3059.
- [3] L. Baudis, *Phys. Dark Univ.* 1 (2012) 94.
- [4] D.Yu. Akimov *et al.*, *Phys. Lett. B* 709 (2012) 14.
- [5] J. Angle *et al.*, XENON Collaboration, *Phys.Rev.Lett.* 100 (2008) 021303.
- [6] E. Aprile *et al.*, XENON100 Collaboration, *Phys. Rev. Lett.* 109 (2012) 181301.
- [7] D.S. Akerib *et al.*, LUX Collaboration (2013) arXiv:1310.8214.
- [8] M. Bossa, DarkSide Collaboration, *JINST* 9 (2014) C01034.
- [9] M.G. Boulay, DEAP Collaboration, *J.Phys.Conf.Ser.* 375 (2012) 012027.
- [10] D.C. Mallin *et al.*, *After LUX: The LZ Program*, (2011) ARXIV:1110.0103.
- [11] L. Baudis, DARWIN Consortium, *J.Phys.Conf.Ser.* 375 (2012) 012028.
- [12] R. Agnese *et al.*, SuperCDMS Collaboration, *Search for Low-Mass WIMPs with SuperCDMS* (2014) ARXIV:1402.7137.
- [13] H. Kraus *et al.*, *PoS IDM2010* (2011) 109.
- [14] P. Cushman *et al.*, *Snowmass CF1 Summary: WIMP Dark Matter Direct Detection* (2013) ARXIV:1310.8327.
- [15] Elena Aprile and Laura Baudis, *Liquid noble gases, in Bertone, G. (ed.): Particle dark matter* (2010) 413.
- [16] D.Yu. Akimov *et al.*, ZEPLIN-III Collaboration, *Nucl.Instrum.Meth.* A623 (2010) 451.
- [17] E. Aprile *et al.*, XENON100, *Astropart. Phys.* 35 (2012) 573.
- [18] Laura Baudis, *PoS IDM2010* (2011) 122.
- [19] L. Baudis *et al.*, *Phys.Rev.* D88 (2013) 115014.
- [20] H. Uchida *et al.*, XMASS-I Collaboration, *PTEP* 6 (2014) 063C01.
- [21] M. Pospelov, A. Ritz and M.B. Voloshin, *Phys.Rev.* D78 (2008) 115012.
- [22] K. Abe *et al.*, XMASS Collaboration, *Phys. Rev. Lett.* 113 (2014) 121301.
- [23] E. Aprile *et al.*, XENON100 Collaboration (2011) *Phys.Rev.* D83 (2011) 082001.
- [24] R.G. Robertson *et al.*, KATRIN Collaboration, *KATRIN: an experiment to determine the neutrino mass from the beta decay of tritium* (2013) ARXIV:1307.5486.
- [25] J.A. Formaggio *et al.*, *Solving for Micro- and Macro-Scale Electrostatic Configurations Using the Robin Hood Algorithm*, ARXIV:1111.5035.
- [26] E. Aprile *et al.*, XENON Collaboration *Lowering the radioactivity of the photomultiplier tubes for the XENON1T dark matter experiment* (2015) arXiv:1503.07698.
- [27] L. Baudis *et al.*, *JINST* 8 (2013) P04026.